

Probing the Small Scale Matter Power Spectrum through Dark Matter Annihilation in the Early Universe

Aravind Natarajan,^{1,2,3,*} Nick Zhu,^{4,5} and Naoki Yoshida^{1,4}

¹*Kavli Institute for the Physics and Mathematics of the Universe (WPI),
The University of Tokyo Institutes for Advanced Study, Kashiwa-no-ha, Chiba, 277-8583, Japan*

²*Department of Physics, Engineering Physics, and Astronomy,
Queen's University, Kingston, Ontario K7L 3N6, Canada*

³*Department of Physics and Astronomy, University of Pennsylvania,
209 South 33rd Street, Philadelphia, PA 19104, USA*

⁴*Department of Physics, University of Tokyo, Bunkyo, Tokyo 113-0033, Japan*

⁵*Department of Astrophysical Sciences, Princeton University, Princeton, NJ 08544*

Recent observations of the cosmic microwave background (CMB) anisotropies and the distribution of galaxies, galaxy clusters, and the Lyman α forest have constrained the shape of the power spectrum of matter fluctuations on large scales $k \lesssim \text{few } h/\text{Mpc}$. We explore a new technique to constrain the matter power spectrum on smaller scales, assuming the dark matter is a Weakly Interacting Massive Particle (WIMP) that annihilates at early epochs. Energy released by dark matter annihilation can modify the spectrum of CMB temperature fluctuations and thus CMB experiments such as Planck have been able to constrain the quantity $f\langle\sigma_a v\rangle/m_\chi \lesssim 1/88 \text{ picobarn} \times c/\text{GeV}$, where f is the fraction of energy absorbed by gas, $\langle\sigma_a v\rangle$ is the annihilation rate assumed constant, and m_χ is the particle mass. We assume the standard scale-invariant primordial matter power spectrum of $P_{\text{prim}}(k) \sim k^{n_s}$ at large scales $k < k_p$, while we adopt the modified power law of $P_{\text{prim}}(k) \sim k_p^{n_s} (k/k_p)^{m_s}$ at small scales. We then aim at deriving constraints on m_s . For $m_s > n_s$, the excess small-scale power results in a much larger number of nonlinear small mass halos, particularly at high redshifts. Dark matter annihilation in these halos releases sufficient energy to partially ionize the gas, and consequently modify the spectrum of CMB fluctuations. We show that the recent Planck data can already be used to constrain the power spectrum on small scales. For a simple model with an NFW profile with halo concentration parameter $c_{200} = 5$ and $f\langle\sigma_a v\rangle/m_\chi = 1/100 \text{ picobarn} \times c/\text{GeV}$, we can limit the mass variance $\sigma_{\text{max}} \lesssim 100$ at the 95% confidence level, corresponding to a power law index $m_s < 1.43(1.63)$ for $k_p = 100$ (1000) h/Mpc . Our results are also relevant to theories that feature a running spectral index.

PACS numbers: 98.80.-k, 95.30.Sf, 98.62.Sb, 95.85.Ry

I. INTRODUCTION

The nature of dark matter is unknown and remains one of the greatest mysteries in astrophysics and cosmology. Weakly Interacting Massive Particles (WIMPs) are one of the leading candidates for the dark matter of the Universe, and large experiments are being conducted to detect WIMP dark matter through direct, indirect, and collider experiments. Some direct detection experiments such as DAMA [1] have observed an annual modulation consistent with the presence of dark matter particles of mass $8 - 15 \text{ GeV}$ interacting with a spin-independent cross section of $0.01 - 0.1 \text{ femtobarn}$. Recent observations of the Milky Way center [2] by the Fermi gamma ray telescope also seem to indicate an excess of gamma rays, consistent with dark matter particles of mass $m_\chi = 31 - 40 \text{ GeV}$ annihilating at a rate $\langle\sigma_a v\rangle = (1.4 - 2.0) \times 10^{-26} \text{ cm}^3/\text{s}$. These exciting results are, however, inconsistent with the XENON [3] and LUX experiments [4], and are also disfavored by the non-detection of dark matter annihilation in the local dwarf galaxies [5, 6].

The cosmic microwave background has been shown to be an excellent probe of WIMP dark matter annihilation at high redshifts [7–11]. Particle annihilation releases and injects energy into the cosmic diffuse gas, resulting in both ionization and heating. Free electrons scatter CMB photons and cause damping in the temperature anisotropy power spectrum at intermediate and small angular scales. Also the CMB polarization power spectrum is boosted at very large scales. Precise measurement of the CMB by Planck, WMAP, ACT, and SPT have already placed tight constraints on dark matter properties [12–16]. Interestingly, the recent results from the Planck collaboration [17] constrain the annihilation parameter $p_{\text{ann}} = f\langle\sigma_a v\rangle/m_\chi < 3.4 \times 10^{-28} \text{ cm}^3\text{s}^{-1}\text{GeV}^{-1} = (1/88.3) \text{ pb} \times c/\text{GeV}$, where f is the fraction of energy absorbed by gas. For realistic values of $f \approx 0.35$ for the $b\bar{b}$ channel [18], and $\langle\sigma_a v\rangle = 0.727 \text{ pb} \times c$ [19], one obtains a bound on the dark matter mass $m_\chi > 22.4 \text{ GeV}$ at the 95% confidence level [44].

The CMB constraints on dark matter particle properties are derived on the assumption that only annihilation of free ‘unbound’ particles contribute to the net energy release, i.e. annihilation of particles bound in nonlinear objects, ‘dark halos’, is not considered. The assumption is appropriate because, in the standard cosmology,

*Electronic address: anat01@me.com

nonlinear objects appear only relatively late, at redshifts $z \sim 30 - 50$. Then the gas density is already small, and CMB photons do not interact with free electrons unless the gas is significantly ionized. Nonlinear halos would be, however, important if they formed much earlier, i.e. at redshifts $z > 100$. Such a case is possible if the primordial density fluctuations have some excess power at small length scales.

The simplest inflationary theories predict a nearly scale invariant primordial curvature power spectrum $P_{\mathcal{R}} \sim k^{n_s-1}$, resulting in a present day matter power spectrum:

$$\begin{aligned} P_m(z, k) &\propto A k^{n_s} T^2(k) \frac{D^2(z)}{D^2(0)} \\ &= P_{\text{prim}}(k) T^2(k) \frac{D^2(z)}{D^2(0)}, \end{aligned} \quad (1)$$

where $P_{\text{prim}}(k) \propto k^{n_s}$ is the primordial matter power spectrum on very large scales $k < 10^{-3} \text{ h/Mpc}$, $T(k)$ is the transfer function, and $D(z)$ is the growth factor. Data from the Wilkinson Microwave Anisotropy Probe (WMAP) and the Atacama Cosmology Telescope (ACT) was used by [20] to reconstruct the matter power spectrum at wavenumbers $0.001 < k < 0.19 \text{ Mpc}^{-1}$. On smaller length scales, one may use the Sloan Digital Sky Survey measurements of the clustering of galaxies to probe scales up to $k \sim 0.2 \text{ h/Mpc}$. On even smaller scales, the flux power spectrum of the Lyman α forest may be used to probe the matter power spectrum for $k < 2 \text{ Mpc}^{-1}$. Unfortunately, at $k \gtrsim 10 \text{ h/Mpc}$, there exist no direct observations of the matter power spectrum. Possible probes of the small scale power spectrum include the use of Type Ia supernova lensing dispersion [21], ultra compact mini halos [22–25], and the dissipation of acoustic waves by Silk damping [26, 27].

In the present paper, we explore a new probe of the primordial density fluctuations on very small scales. Let us consider a simple power-law for the matter power spectrum at $k > k_p$:

$$\begin{aligned} P_{\text{prim}} &= A k^{n_s} & k \leq k_p \\ &= A k_p^{n_s} (k/k_p)^{m_s} & k > k_p, \end{aligned} \quad (2)$$

which is consistent with all available observations provided the pivot wavenumber k_p is large enough, say $k_p \gtrsim 10 \text{ h/Mpc}$. Essentially, we examine if there is excess power on the relevant small length scales through energy injection from dark matter annihilation in the early universe. The basic idea is as follows. The mass variance $\sigma^2(z, M)$ is computed by integrating the dimensionless power spectrum $\Delta^2(k) = k^3 P(k)/2\pi^2$ over a window function:

$$\sigma^2(z, M) = \frac{D^2(z)}{D^2(0)} \int \frac{dk}{k} \frac{k^3 P(k)}{2\pi^2} W^2(kR). \quad (3)$$

The normalization constant A is chosen such that $\sigma_8 = 0.8$, where σ_8 is the root mean square mass fluctuation in a sphere of radius $8 \text{ Mpc}/h$. The linear growth function of matter overdensities is denoted by $D(z)$. With

the Planck cosmology, we find $D(z=0) = 0.757$. The window function $W(kR)$ for comoving scale R is conveniently given by

$$W(x) = \frac{3 [\sin x - x \cos x]}{x^3}, \quad (4)$$

and R is the comoving radius that encloses a mass M . Fig. 1(a) shows the matter power spectrum for the standard cosmology (solid lines, black) computed using the Eisenstein-Hu transfer function [28, 29]. Also plotted are curves for $n_s = 0.96$, and the modified power law of Eq. 2, for $m_s = 1.1, 1.2$, and 1.5 . An exponential cutoff is imposed at the free streaming scale $k_{\text{fs}} \sim 10^6 \text{ h/Mpc}$ [30–32], to account for the finite velocity dispersion of WIMP dark matter, and to make the integral in Eq. 3 finite. This ensures that there is a minimum halo mass $M_{\text{min}} \sim 10^{-6} M_{\odot}$. Panel (b) shows the standard deviation σ of density fluctuations, for these models. Note that $\sigma_{\text{max}} = \sigma(M_{\text{min}})$ is very sensitive to m_s , although $\sigma_8 = 0.8$ for all models.

II. DARK MATTER ANNIHILATION IN HALOS

Consider an overdensity of weakly interacting dark matter particles. The number of WIMPs in a volume δV is $(\rho_{\chi}/m_{\chi})\delta V$, where ρ_{χ} is the density of WIMPs, and the probability of WIMP annihilation in a time δt is $\langle \sigma_a v \rangle \delta t$. The number of WIMP annihilations per unit time per unit volume is then equal to $\langle \sigma_a v \rangle \rho_{\chi}^2/m_{\chi}^2$. Since each annihilation releases m_{χ} of energy per particle, the total energy released per unit time per unit volume equals

$$\frac{dE}{dt dV} = \frac{\langle \sigma_a v \rangle}{m_{\chi}} \rho_{\chi}^2. \quad (5)$$

The energy per unit time due to particle annihilation in a bound halo of radius r_{200} is obtained by integrating Eq. 5 over the halo volume:

$$\frac{dE}{dt} = \frac{\langle \sigma_a v \rangle}{m_{\chi}} \int_0^{r_{200}} dr 4\pi r^2 \rho_{\text{halo}}^2(r). \quad (6)$$

r_{200} is the radius at which the mean density enclosed equals 200 times the cosmological mean at the redshift of formation of the halo:

$$\frac{3M}{4\pi r_{200}^3} = 200\rho_0[1 + z_f(M)]^3, \quad (7)$$

where ρ_0 is the mean dark matter density at the present epoch ($z=0$), and $z_f(M)$ is the formation redshift of a halo of mass M . We may parameterize the halo density profile as:

$$\rho(x) = \frac{\rho_s}{x^{\alpha}(1+x)^{\beta}}, \quad (8)$$

where $x = r/r_s$ is a dimensionless radius. ρ_s and r_s are constants for a halo. The well known Navarro-Frenk-White (NFW) [33] form is obtained when we set $\alpha = 1$ and $\beta = 2$.

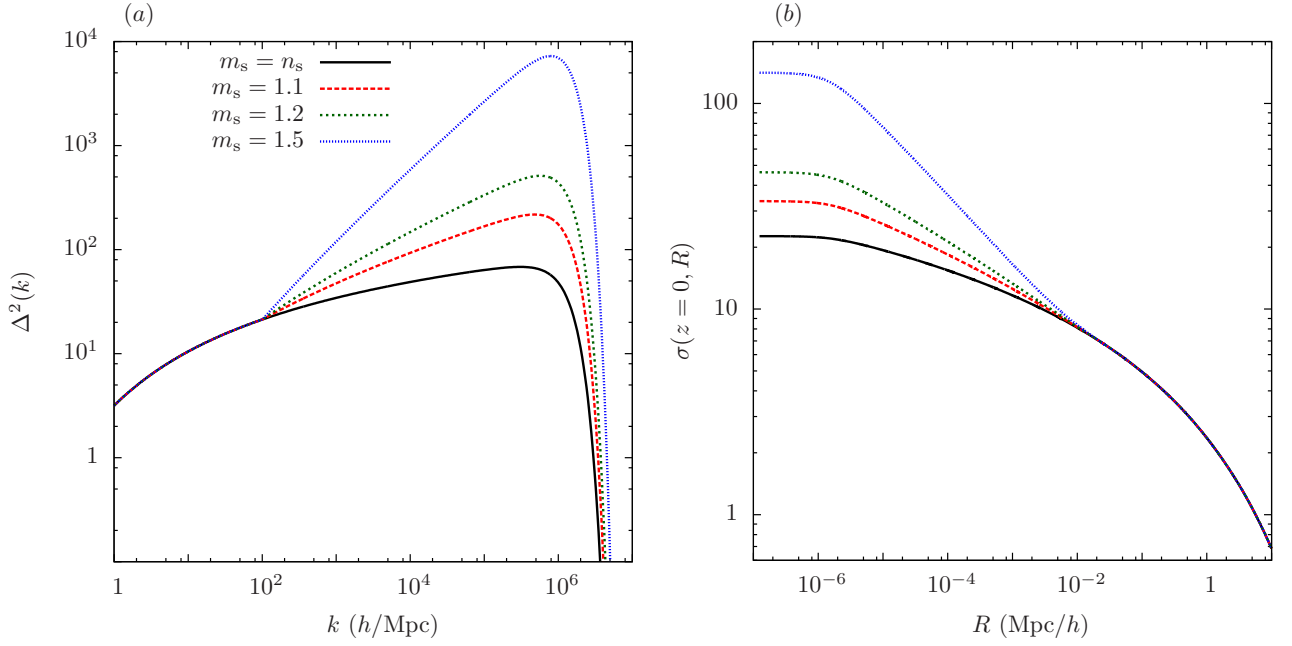


FIG. 1: We plot the dimensionless matter power spectrum for the standard cosmology (solid, black), as well as for the cases $m_s = 1.1, 1.2$, and 1.5 , for $k_p = 100 h/\text{Mpc}$ (Panel a). An exponential cut-off is applied at the free streaming scale k_{fs} chosen to be $10^6 h/\text{Mpc}$. Panel (b) shows the corresponding standard deviation σ of fluctuations normalized to $\sigma_8 = 0.8$.

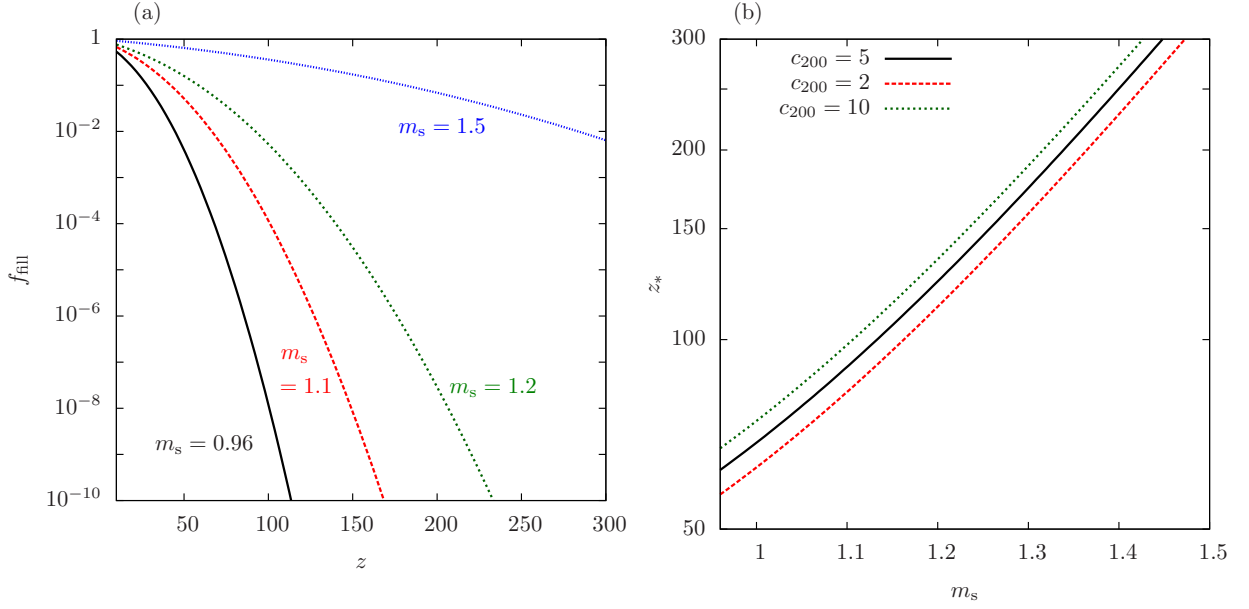


FIG. 2: We plot the filling fraction f_{fill} for different values of m_s , for $k_p = 100 h/\text{Mpc}$ (Panel a). The difference appears small at $z = 0$, but is substantial for large z . Panel (b) shows the redshift z_* below which the halo contribution exceeds the free particle contribution. It is not very sensitive to the concentration parameter because of the exponential decrease of f_{fill} with z .

We define the concentration parameter as:

$$c_{200} = \frac{r_{200}}{r_s}. \quad (9)$$

Note that we have defined r_{200} and c_{200} at the formation epoch. We may now express ρ_s and r_s in terms of M and

c_{200} . Then the rate of energy release (Eq. 6) is

$$\frac{dE_{\text{halo}}}{dt} = \frac{\langle \sigma_a v \rangle}{m_\chi} \frac{200}{3} M \rho_0 [1 + z_f(M)]^3 f_{\text{conc}}(c_{200}), \quad (10)$$

where $f_{\text{conc}}(c_{200})$ is calculated for the density profile with concentration parameter c_{200} as

$$f_{\text{conc}} = \frac{c_{200}^3 \int_\epsilon^{c_{200}} dx x^{2-2\alpha} (1+x)^{-2\beta}}{\left[\int_0^{c_{200}} dx x^{2-\alpha} (1+x)^{-\beta} \right]^2}. \quad (11)$$

The lower limit ϵ is required when the index $\alpha > 1.5$. For the NFW profile with $\alpha = 1$ and $\beta = 2$, we can set $\epsilon = 0$, and then Eq. 11 is integrated analytically to yield

$$f_{\text{conc}} = \frac{c_{200}^3}{3} \frac{1 - (1 + c_{200})^{-3}}{[\ln(1 + c_{200}) - c_{200}(1 + c_{200})^{-1}]^2}. \quad (12)$$

A halo of mass $\sim 10^{12} M_\odot$ similar to the Milky Way is expected to have a concentration parameter $c_{200} \sim 10$ [34]. Earth-mass microhalos, on the other hand, are not expected to have large concentration parameters. [35] found concentration parameters $c_{200} \lesssim 3$ for such very small halos. We simply assume a constant $c_{200} = 5$ independent of mass.

To evaluate Eq. 10, we need to determine the redshift of formation of the halo. Following the Press-Schechter formalism [36], we assume that the probability of finding a halo of mass M at a redshift z is $\propto \exp[-\delta_c^2/2\sigma^2(M, z)]$, where $\delta_c = 1.686$ is the threshold for halo formation in linear theory. We can then estimate the averaged quantity:

$$\left\langle \left[\frac{1 + z_f(M)}{1 + z} \right]^3 \right\rangle = \frac{\frac{1}{x_*^3} \int_{x_*}^\infty dx x^3 e^{-x^2}}{\int_{x_*}^\infty dx e^{-x^2}}, \quad (13)$$

where $x_* = \delta_c/\sqrt{2}\sigma(z, M)$. Note that Eq. 13 approaches unity for large halo masses and large redshifts.

The total energy due to WIMP annihilation per unit time and per unit volume may be obtained by integrating Eq. 10 over the halo distribution:

$$\begin{aligned} \frac{dE}{dt dV} &= (1+z)^3 \int_{M_{\min}}^\infty dM \frac{dN}{dM} \frac{dE_{\text{halo}}}{dt} \\ &= \frac{\langle \sigma_a v \rangle}{m_\chi} \frac{200 \rho_0}{3} f_{\text{conc}}(c_{200}) (1+z)^6 \\ &\quad \times \int_{M_{\min}}^\infty dM M \frac{dN}{dM} \left\langle \left[\frac{1 + z_f(M)}{1 + z} \right]^3 \right\rangle \end{aligned} \quad (14)$$

The comoving number density of halos is calculated from, for instance, the Press-Schechter mass function as

$$\frac{dN}{dM} = \sqrt{\frac{2}{\pi}} \rho_0 \left| \frac{1}{\sigma} \frac{d\sigma}{dM} \right| \frac{\delta_c}{\sigma} \exp \left[-\frac{\delta_c^2}{2\sigma^2} \right]. \quad (15)$$

We have simplified the mass function by setting ρ_0 equal to the dark matter density, rather than the matter density. Let us define the filling factor $f_{\text{fill}}(z)$ as the fraction

of matter in bound halos:

$$\begin{aligned} f_{\text{fill}}(z) &= \frac{1}{\rho_0} \int_{M_{\min}}^\infty dM M \frac{dN}{dM} \\ &= \text{erfc} \left[\frac{\delta_c D(0)(1+z)}{\sqrt{2}\sigma(0, M)} \right], \end{aligned} \quad (16)$$

We also define the quantify $\zeta(z)$ by

$$f_{\text{fill}}(z) \zeta(z) = \frac{1}{\rho_0} \int_{M_{\min}}^\infty dM M \frac{dN}{dM} \left\langle \left[\frac{1 + z_f(M)}{1 + z} \right]^3 \right\rangle. \quad (17)$$

which is larger than 1 at low redshifts but approaches 1 for large z . Fig. 2(a) shows the filling fraction for different choices of m_s . We set $k_p = 100 h/\text{Mpc}$ as our fiducial model parameter. The black curve shows the case $m_s = n_s = 0.96$, i.e. the standard power law. Clearly, the filling factor can be many orders of magnitude larger at high redshifts if $m_s > n_s$.

It is also interesting to compute z_* , the redshift below which the nonlinear halo contribution exceeds the free particle contribution. Fig. 2(b) shows z_* calculated for different values of the concentration parameter. It is not very sensitive to the concentration parameter due to the exponential decrease of the mass function. For the standard matter power spectrum, halos are only important at redshifts $z \lesssim 50$. However, for $m_s = 1.5$, halos contribute significantly even at $z = 300$.

At high redshifts, we may make the ‘‘on the spot’’ approximation when calculating the net energy input to the gas. Namely, we may safely ignore the propagation of high energy annihilation products from the redshift of emission to the redshift of absorption. The net energy absorbed per atom per unit time at a redshift z is given by:

$$\begin{aligned} \xi(z) &= \frac{f}{n_b(z)} \frac{dE}{dt dV} \\ &= \frac{f \langle \sigma_a v \rangle \bar{m}}{m_\chi} \left(\frac{\rho_{\text{crit}}}{h^2} \right) \frac{(\Omega_\chi h^2)^2}{\Omega_b h^2} (1+z)^3 \\ &\quad \times \left[1 - f_{\text{fill}}(z) + \frac{200}{3} f_{\text{conc}}(c_{200}) f_{\text{fill}}(z) \zeta(z) \right] \end{aligned} \quad (18)$$

where f is the fraction of energy absorbed by the gas, $n_b(z)$ is the baryon number density, and \bar{m} is the mean nucleon mass, assuming 76% hydrogen and 24% helium. Ω_b , Ω_χ , and Ω_m are the baryon, dark matter, and total matter fractions at the present epoch.

III. CMB CONSTRAINT

In the previous section, we computed the rate of energy release due to dark matter annihilation in halos. The fraction f of the released energy is absorbed by the gas, and a fraction $\eta_{\text{ion}}(x_{\text{ion}})$ of this energy goes into ionization, whereas a fraction $\eta_{\text{heat}}(x_{\text{ion}})$ goes into heating.

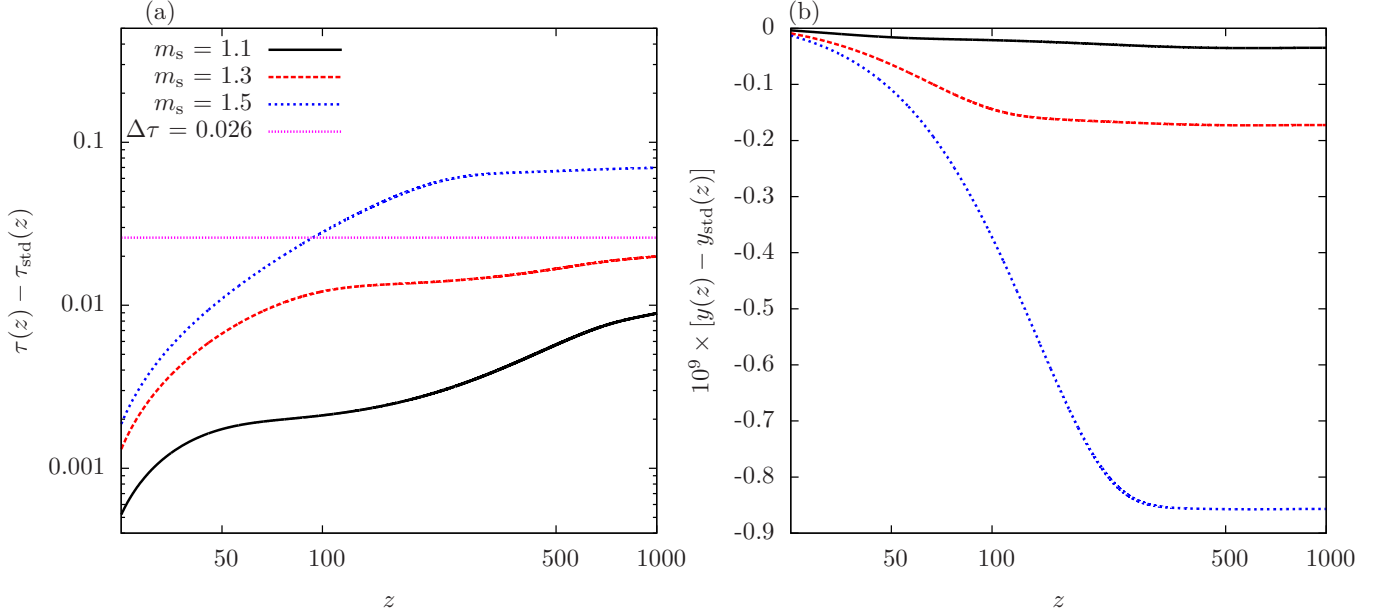


FIG. 3: The excess optical depth due to dark matter annihilation including the contribution from nonlinear haloes, for $m_s = 1.1, 1.3, 1.5$ (Panel a). The magenta line shows $\Delta\tau = 0.026$ which is the maximum allowed excess optical depth above $z = 6$ (see text). Panel (b) shows the corresponding excess Compton y parameter due to dark matter annihilation as a function of z .

We use the results obtained by [37] to estimate η_{ion} and η_{heat} . The ionization and temperature evolution follow the equations [16]:

$$\begin{aligned}
 -(1+z)H(z)\frac{dx_{\text{ion}}(z)}{dz} &= \mu[1-x_{\text{ion}}(z)]\eta_{\text{ion}}(z)\xi(z) \\
 &\quad - n(z)x_{\text{ion}}^2(z)\alpha(z) \\
 -(1+z)H(z)\frac{dT(z)}{dz} &= -2T(z)H(z) + \frac{2\eta_{\text{heat}}(z)}{3k_b}\xi(z) \\
 &\quad + \frac{x_{\text{ion}}(z)[T_\gamma(z) - T(z)]}{t_c(z)}. \quad (19)
 \end{aligned}$$

$\mu \approx 0.07 \text{ eV}^{-1}$ is the inverse of the average ionization energy per atom, neglecting double ionization of helium. In the above equations, α is the case-B recombination coefficient, T_γ is the CMB temperature, k_b is Boltzmann's constant, and t_c is the Compton cooling time scale $\approx 1.44 \text{ Myr} [30/(1+z)]^4$. The last term in the temperature evolution equation accounts for the transfer of energy between free electrons and the CMB by Compton scattering [38–40]. In the temperature coupling term, we assume $x_{\text{ion}} \ll 1$ and ignore the helium number fraction. In practice, we compute x_{ion} and T_{gas} using a modified version of the publicly available RECFAST program [39, 40].

CMB photons scatter off free electrons that are present due to partial ionization of the gas. Thomson scattering of the CMB causes damping of the temperature anisotropy TT power spectrum, as well as a boost in the large angle EE polarization power spectrum [16]. The scattering is quantified by means of the optical depth de-

fined as the scattering cross section times the free electron density integrated along the line of sight:

$$\tau(z_1, z) = \int dt c \sigma_T n_e(z) \quad (20)$$

where σ_T is the Thomson cross section. We also calculate the ‘excess’ contribution as

$$\begin{aligned}
 \tau - \tau_{\text{std}} &= \frac{c\sigma_T (\rho_{\text{crit}}/h^2)}{H_{100} \bar{m}} \frac{\Omega_b h^2}{\sqrt{\Omega_m} h^2} \\
 &\quad \times \int_{z_1}^z dz (1+z)^{1/2} \Delta x(z) \quad (21)
 \end{aligned}$$

with $H_{100} = 100 \text{ km/s/Mpc}$ and $\Delta x = x_{\text{ion}} - x_{\text{std}}$, where x_{std} denotes the standard recombination history (i.e. without dark matter annihilation, and $m_s = n_s$). We have ignored dark energy, and therefore, the above equation holds true for $z_1 \gg 0$.

We see that even small changes in x_{ion} at high redshifts can boost the total optical depth due to the $\sqrt{1+z}$ term. One may also hope to constrain dark matter annihilation by measuring the spectral distortion of the CMB, quantified by the Compton y parameter [41, 42]:

$$\begin{aligned}
 y &= \int d\tau \frac{k_b [T(z) - T_\gamma(z)]}{m_e c^2} \\
 y - y_{\text{std}} &\approx \frac{c\sigma_T (\rho_{\text{crit}}/h^2)}{H_{100} \bar{m}} \frac{\Omega_b h^2}{\sqrt{\Omega_m} h^2} \frac{k_b}{m_e c^2} \\
 &\quad \times \int_{z_1}^z dz (1+z)^{1/2} [x_{\text{std}} \Delta T + \Delta x (T_{\text{std}} - T_\gamma)], \quad (22)
 \end{aligned}$$

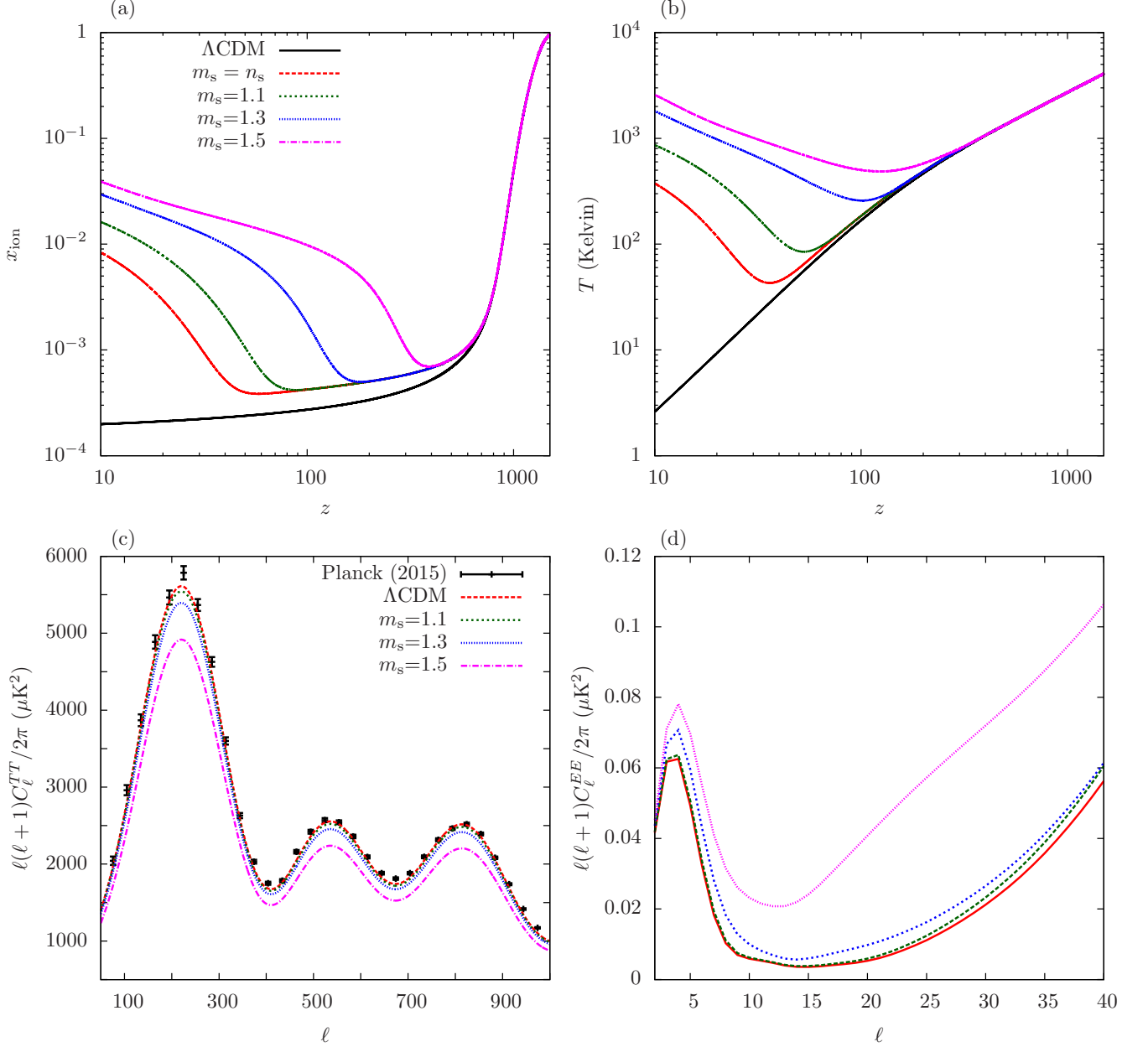


FIG. 4: The top panels (a) and (b) show the ionization and temperature history of the Universe. The black curve is plotted for the standard ΛCDM cosmology, i.e. ignoring dark matter annihilation. The red curve ($m_s = n_s$) is for a standard power spectrum, but includes the effect of dark matter annihilation. The green, blue, and magenta curves are plotted for the modified power law of Eq. 2. The bottom panels (c) and (d) show the temperature and polarization power spectra for the four models.

where $\Delta T(z) = T(z) - T_{\text{std}}(z)$, and as before, T_{std} represents the gas temperature in the standard ΛCDM scenario.

Fig. 3(a) shows the excess optical depth due to dark matter annihilation with $m_s = 1.1, 1.3$, and 1.5 , with dark matter mass $m_\chi = 100$ GeV, and concentration parameter $c_{200} = 5$. Assuming the total optical depth measured by Planck $\tau \approx 0.066$ [17] and full ionization up to $z = 6$, we find that the excess optical depth $\Delta\tau \lesssim 0.026$,

which excludes large values of m_s . The Compton y parameter is less constraining because it is weighted towards large z when the gas temperature is close to the CMB temperature due to efficient Compton scattering. The planned PIXIE mission can constrain $|y| < 2 \times 10^{-9}$ [42], and may exclude very large values of m_s at the relevant length-scales.

Fig. 4 shows the evolution of the ionization fraction (Panel a) and the gas temperature (Panel b), for dif-

ferent values of m_s . We assume $f\langle\sigma_a v\rangle/m_\chi = 1/100$ pb×c/GeV for the figure. The black curve is plotted for the standard Λ CDM, i.e. ignoring dark matter annihilation. The red curve is plotted for the standard power law, but with accounting for dark matter annihilation. The green, blue, and magenta curves are the results for $m_s = 1.1, 1.3$, and 1.5 , respectively. The effect on the CMB TT and EE power spectra is shown in Panels (c) and (d). For large m_s , significant damping is caused on the TT power spectrum, as clearly seen in Panel (c). Also plotted in (c) are the TT power measurement from Planck. It might appear that large values of m_s are already excluded at high significance. However, the amplitude of the CMB power spectrum is determined by $\sim A_s \exp -2\tau$. While the optical depth τ is increased by ionization by dark matter annihilation, the effect is almost fully degenerate with the amplitude of the primordial curvature power spectrum A_s , except on very large scales that were outside the horizon at the time of particle annihilation. Therefore, the TT power spectrum alone cannot be used to place constraints on dark matter annihilation, but the degeneracy is broken by using information of the CMB polarization, because Thomson scattering causes a *boost* in the large angle polarization power spectrum. A second technique to break the degeneracy is through the measurement of gravitational lensing of the CMB by large scale structure. The Planck experiment has recently measured the lensing potential at the 40σ level [43]. Measurement of the gravitational lensing of the CMB places constraints on the combination $\sigma_8\Omega_m^{0.25} = 0.591 \pm 0.021$. Since other constraints exist for Ω_m , the measurement of gravitational lensing places a bound on σ_8 , and hence on A_s . Gravitational lensing thus breaks the degeneracy between A_s and τ . The recent results from Planck give us $\log(10^{10}A_s) = 3.064 \pm 0.023$, and $\tau = 0.066 \pm 0.012$, which we can now be used to place bounds on the root mean square mass fluctuation σ_{\max} , and hence on the power law index m_s .

We consider a number of models with different m_s and calculate σ_{\max} . We also compute the corresponding ionization history and the CMB power spectra using a modified version of the CAMB software, assuming $p_{\text{ann}} = f\langle\sigma_a v\rangle/m_\chi = (1/100)$ pb×c/GeV. For each model, we fit the theoretical power spectra to the observed TT power spectrum, by modifying the quantity $A_s e^{-2\tau}$. By means of Montecarlo simulations, we obtain a bound on the combination $A_s e^{-2\tau} = 1.872 \pm 0.101$. The 2σ upper bound on $A_s e^{-2\tau}$ results in a corresponding bound on the standard deviation of mass fluctuations: $\sigma_{\max} < 100$ at the 2σ level. This finally translates to a bound on the power law index: $m_s < 1.43(1.63)$ for $k_p = 100$ (1000) h/Mpc .

IV. CONCLUSIONS

We have proposed a new probe of the matter power spectrum on very small scales, through the effect of dark

matter annihilation on the thermal evolution and on the ionization history of the inter-galactic gas. We have considered a simple modification to the standard power law, for the primordial power spectrum: $P_{\text{prim}}(k) \sim k_p^{n_s} (k/k_p)^{m_s}$, where $m_s \geq n_s$. Such a power law is acceptable provided k_p is large enough, e.g. $k_p > 10$ h/Mpc . The form of the root mean square mass fluctuation σ has been calculated as a function of the power law index m_s . The maximum value $\sigma_{\max} = \sigma(M_{\min})$ varies significantly with m_s . One may expect a $1-\sigma$ fluctuation to enter the non-linear regime when $1+z \approx \sigma_{\max}/\delta_c D(0)$. We have then computed the filling fraction (the fraction of dark matter bound in nonlinear halos) as a function of redshift. For large m_s , there are many orders of magnitude more halos at $z > 100$. For the standard power spectrum power law, halos are only important for $z \lesssim 50$. On the other hand, when $m_s \sim 1.5$, halos provide the dominant contribution to total dark matter annihilation rate even at $z = 300$.

We derived an explicit expression for the energy injected per unit gas atom per unit time at a redshift z . A large contribution from dark matter halos at $z \sim 300$ can significantly alter the spectrum of CMB anisotropies. We computed the CMB power spectra using the CAMB code, for a fiducial dark matter annihilation cross-section of $p_{\text{ann}} = f\langle\sigma_a v\rangle/m_\chi = (1/100)$ pb×c/GeV. We used the Planck (2015) TT power spectrum data to test theoretical models. The current data already excludes a root mean square fluctuation $\sigma_{\max} = \sigma(M_{\min}) \gtrsim 100$ at the 2σ level. The bound on σ_{\max} may be expressed as a constraint on the power law index on small scales: We exclude $m_s > 1.43(1.63)$ for $k_p = 100$ (1000) h/Mpc .

Acknowledgments

A.N. acknowledges funding from the Japan Society for the Promotion of Science (JSPS) and the Kavli Institute for the Physics and Mathematics of the Universe (IPMU). A.N. is grateful to Queen's University and the University of Pennsylvania for hospitality and funding. The authors thank David Spergel for fruitful discussions, and also for suggesting the use of the Planck measurements of the optical depth and the fluctuation amplitude. NZ is grateful for the hospitality of David Spergel and the Department of Astrophysical Sciences at Princeton University. NZ's visit was supported by the University of Tokyo-Princeton strategic partnership grant.

-
- [1] R. Bernabei, P. Belli, F. Cappella, V. Caracciolo, R. Cerulli, C. J. Dai, A. d'Angelo, S. d'Angelo, A. Di Marco, H. L. He, *et al.*, Nuclear Instruments and Methods in Physics Research A **742**, 177 (Apr. 2014), 1403.1404.
 - [2] T. Daylan, D. P. Finkbeiner, D. Hooper, T. Linden, S. K. N. Portillo, N. L. Rodd, and T. R. Slatyer, ArXiv e-prints (Feb. 2014), 1402.6703.
 - [3] E. Aprile, M. Alfonsi, K. Arisaka, F. Arneodo, C. Balan, L. Baudis, B. Bauermeister, A. Behrens, P. Beltrame, K. Bokeloh, *et al.*, Physical Review Letters **109**(18), 181301, 181301 (Nov. 2012), 1207.5988.
 - [4] D. S. Akerib, H. M. Araújo, X. Bai, A. J. Bailey, J. Balajthy, S. Bedikian, E. Bernard, A. Bernstein, A. Bolozdynya, A. Bradley, *et al.*, Physical Review Letters **112**(9), 091303, 091303 (Mar. 2014).
 - [5] A. Geringer-Sameth and S. M. Koushiappas, Physical Review Letters **107**(24), 241303, 241303 (Dec. 2011), 1108.2914.
 - [6] M. Ackermann, M. Ajello, A. Albert, W. B. Atwood, L. Baldini, J. Ballet, G. Barbiellini, D. Bastieri, K. Bechtol, R. Bellazzini, *et al.*, Physical Review Letters **107**(24), 241302, 241302 (Dec. 2011), 1108.3546.
 - [7] X. Chen and M. Kamionkowski, Phys. Rev. D **70**(4), 043502, 043502 (Aug. 2004), astro-ph/0310473.
 - [8] N. Padmanabhan and D. P. Finkbeiner, Phys. Rev. D **72**(2), 023508, 023508 (Jul. 2005), astro-ph/0503486.
 - [9] A. Natarajan and D. J. Schwarz, Phys. Rev. D **78**(10), 103524, 103524 (Nov. 2008), 0805.3945.
 - [10] A. Natarajan and D. J. Schwarz, Phys. Rev. D **80**(4), 043529, 043529 (Aug. 2009), 0903.4485.
 - [11] A. Natarajan and D. J. Schwarz, Phys. Rev. D **81**(12), 123510, 123510 (Jun. 2010), 1002.4405.
 - [12] S. Galli, F. Iocco, G. Bertone, and A. Melchiorri, Phys. Rev. D **80**(2), 023505, 023505 (Jul. 2009), 0905.0003.
 - [13] S. Galli, F. Iocco, G. Bertone, and A. Melchiorri, Phys. Rev. D **84**(2), 027302, 027302 (Jul. 2011), 1106.1528.
 - [14] G. Hütsi, J. Chluba, A. Hektor, and M. Raidal, Astron. Astrophys. **535**, A26, A26 (Nov. 2011), 1103.2766.
 - [15] G. Giesen, J. Lesgourgues, B. Audren, and Y. Ali-Haïmoud, Journal of Cosmology and Astroparticle Physics **12**, 8, 008 (Dec. 2012), 1209.0247.
 - [16] A. Natarajan, Phys. Rev. D **85**(8), 083517, 083517 (Apr. 2012), 1201.3939.
 - [17] Planck Collaboration, P. A. R. Ade, N. Aghanim, M. Arnaud, M. Ashdown, J. Aumont, C. Baccigalupi, A. J. Banday, R. B. Barreiro, J. G. Bartlett, *et al.*, ArXiv e-prints (Feb. 2015), 1502.01589.
 - [18] T. R. Slatyer, N. Padmanabhan, and D. P. Finkbeiner, Phys. Rev. D **80**(4), 043526, 043526 (Aug. 2009), 0906.1197.
 - [19] T. Han, Z. Liu, and A. Natarajan, Journal of High Energy Physics **11**, 8, 8 (Nov. 2013), 1303.3040.
 - [20] R. Hlozek, J. Dunkley, G. Addison, J. W. Appel, J. R. Bond, C. Sofia Carvalho, S. Das, M. J. Devlin, R. Dünner, T. Essinger-Hileman, *et al.*, Astrophys. J. **749**, 90, 90 (Apr. 2012), 1105.4887.
 - [21] I. Ben-Dayan and T. Kalaydzhyyan, Phys. Rev. D **90**(8), 083509, 083509 (Oct. 2014), 1309.4771.
 - [22] A. S. Josan and A. M. Green, Phys. Rev. D **82**(8), 083527, 083527 (Oct. 2010), 1006.4970.
 - [23] Y. Yang, G. Yang, and H. Zong, Phys. Rev. D **87**(10), 103525, 103525 (May 2013), 1305.4213.
 - [24] F. Li, A. L. Erickcek, and N. M. Law, Phys. Rev. D **86**(4), 043519, 043519 (Aug. 2012), 1202.1284.
 - [25] T. Bringmann, P. Scott, and Y. Akrami, Phys. Rev. D **85**(12), 125027, 125027 (Jun. 2012), 1110.2484.
 - [26] T. Nakama, T. Suyama, and J. Yokoyama, Physical Review Letters **113**(6), 061302, 061302 (Aug. 2014), 1403.5407.
 - [27] D. Jeong, J. Pradler, J. Chluba, and M. Kamionkowski, Physical Review Letters **113**(6), 061301, 061301 (Aug. 2014), 1403.3697.
 - [28] D. J. Eisenstein and W. Hu, Astrophys. J. **496**, 605 (Mar. 1998), astro-ph/9709112.
 - [29] D. J. Eisenstein and W. Hu, Astrophys. J. **511**, 5 (Jan. 1999), astro-ph/9710252.
 - [30] A. M. Green, S. Hofmann, and D. J. Schwarz, Mon. Not. R. Astron. Soc. **353**, L23 (Sep. 2004), astro-ph/0309621.
 - [31] A. M. Green, S. Hofmann, and D. J. Schwarz, Journal of Cosmology and Astroparticle Physics **8**, 3, 003 (Aug. 2005), astro-ph/0503387.
 - [32] A. Loeb and M. Zaldarriaga, Phys. Rev. D **71**(10), 103520, 103520 (May 2005), astro-ph/0504112.
 - [33] J. F. Navarro, C. S. Frenk, and S. D. M. White, Astrophys. J. **490**, 493 (Dec. 1997), arXiv:astro-ph/9611107.
 - [34] A. V. Macciò, A. A. Dutton, F. C. van den Bosch, B. Moore, D. Potter, and J. Stadel, Mon. Not. R. Astron. Soc. **378**, 55 (Jun. 2007), astro-ph/0608157.
 - [35] J. Diemand, B. Moore, and J. Stadel, Nature (London) **433**, 389 (Jan. 2005), astro-ph/0501589.
 - [36] W. H. Press and P. Schechter, Astrophys. J. **187**, 425 (Feb. 1974).
 - [37] S. R. Furlanetto and S. J. Stoeve, Mon. Not. R. Astron. Soc. **404**, 1869 (Jun. 2010), 0910.4410.
 - [38] R. Weymann, Physics of Fluids **8**, 2112 (Nov. 1965).
 - [39] S. Seager, D. D. Sasselov, and D. Scott, Astrophys. J. Suppl. **128**, 407 (Jun. 2000), astro-ph/9912182.
 - [40] S. Seager, D. D. Sasselov, and D. Scott, Astrophys. J. Lett. **523**, L1 (Sep. 1999), astro-ph/9909275.
 - [41] J. Chluba and R. A. Sunyaev, Mon. Not. R. Astron. Soc. **419**, 1294 (Jan. 2012), 1109.6552.
 - [42] A. Kogut, D. J. Fixsen, D. T. Chuss, J. Dotson, E. Dwek, M. Halpern, G. F. Hinshaw, S. M. Meyer, S. H. Moseley, M. D. Seiffert, *et al.*, Journal of Cosmology and Astroparticle Physics **7**, 25, 025 (Jul. 2011), 1105.2044.
 - [43] Planck Collaboration, P. A. R. Ade, N. Aghanim, M. Arnaud, M. Ashdown, J. Aumont, C. Baccigalupi, A. J. Banday, R. B. Barreiro, J. G. Bartlett, *et al.*, ArXiv e-prints (Feb. 2015), 1502.01591.
 - [44] It must be noted that the CMB bound only applies for *s*-wave (velocity independent) annihilation.